

Compact Model for the Electronic Properties of Edge-Disordered Graphene Nanoribbons

Arash Yazdanpanah Goharrizi^{1,2}, Mahdi Pourfath², Morteza Fathipour¹, and Hans Kosina²

¹University of Tehran, Electrical Engineering

North Kargar Ave, Tehran, Iran, PO BOX 16315-1355

²Technische Universität Wien, Institute for Microelectronics

Gußhausstraße 27–29/E360, A-1040 Wien, Austria

email: pourfath@iue.tuwien.ac.at

Abstract

The electronic properties of graphene nano-ribbons in the presence of line-edge roughness scattering are studied. The conductance, the mean free path, and the localization length of carriers are analytically derived using an effective mass model for the band structure. The model developed provides a deep insight into the operation of graphene nanoribbon devices in the presence of line-edge roughness. The effects of geometrical parameters on the conductance of graphene nanoribbons are estimated assuming a diffusive transport regime. However, in the presence of disorder, localization of carriers can occur, which can significantly reduce the conductance of the device. The effect of localization on the conductance of rough nanoribbons is studied analytically. Since this regime is not suitable for the operation of electronic devices, one can employ these models to obtain critical geometrical parameters to suppress the localization of carriers in graphene nanoribbon devices.

1. Introduction

Graphene, a planar single sheet of carbon atoms arranged in a honeycomb lattice, has recently attracted major attention due to its remarkable electronic properties [1–7]. One of the most interesting characteristics of graphene is the high carrier mobility, even at room temperature [8]. In order to use graphene, which is a gap less material, for electronic applications a gap should be induced. By applying geometrical confinement an energy gap can be achieved. These structures are called graphene nanoribbons (GNRs). The band gap of GNRs depends on the chirality and the width of ribbon. To obtain a band gap larger than 0.1eV, which is essential for electronic applications, the width of the ribbon must be scaled below 10nm. However, at this scale the mobility of GNRs can be degraded due to the presence of the line-edge roughness. Experimental data show that the line-edge roughness is the dominant scattering mechanism for GNRs with a width below 50nm [9]. With increasing roughness amplitude or length of the ribbon the transport regime can be changed from diffusive to localization. In this regime carrier transport occurs mostly by tun-

neling between localized states along the device. In the diffusive regime the conductance of the ribbon decreases linearly with device length, whereas, in the localization regime it decreases exponentially with the ribbon's length [10]. For the given roughness parameters, one can avoid this regime by appropriately selecting geometrical parameters. Therefore, for designing GNR based devices and optimizing their characteristics, the role of geometrical and roughness parameters on the functionality of such devices must be clearly understood. In this work, new models for the mean free path and the localization length have been analytically derived. Our model can also predict the appearance of localization in GNRs for the given geometrical parameters. Excellent agreement with experimental data indicates the validity of our compact model.

2. The Electronic Band Structure

It has been shown that a three nearest neighbor tight binding approximation along with an edge-distortion correction can accurately predict the band structure of GNRs [11]. The band structure of an armchair GNR can be written as [12]:

$$E_n^\pm(k_x) \approx \pm \sqrt{(E_{G,n}/2)^2 + (\hbar v_n)^2 k_x^2}, \quad (1)$$

with

$$E_{G,n} \equiv 2[\gamma_1 (2 \cos(n\theta) + 1) + \gamma_3 (2 \cos(2n\theta) + 1) + \frac{4(\gamma_3 + \Delta\gamma_1)}{N+1} \sin^2(n\theta)] \quad (2)$$

and

$$v_n^2 = \left(\frac{3a_{cc}}{\hbar}\right)^2 \left[-\frac{1}{2}\gamma_1 \cos(n\theta) \left\{ \gamma_1 + \gamma_3 (2 \cos(2n\theta) + 1) + \frac{4(\gamma_3 + \Delta\gamma_1)}{N+1} \sin^2(n\theta) \right\} - \gamma_3 \left\{ \gamma_1 + 2\gamma_3 \cos(2n\theta) + \frac{4(\gamma_3 + \Delta\gamma_1)}{N+1} \sin^2(n\theta) \right\} \right] \quad (3)$$

$$\theta = \frac{\pi}{N+1} \quad (4)$$

In Eq. (1), + and - represent the conduction and the valence bands, respectively, N is the total number of A and B -type carbon atoms in each chain of the ribbon (see Fig. 1), $n = 1, \dots, N$ denotes the subband index, and $E_{G,n}$ is the band gap and $E_{C,n}$ the band edge energy of the n th subband. The first and the third nearest neighbor hopping parameters are $\gamma_1 \approx -3.2\text{eV}$ and $\gamma_3 \approx -0.3\text{eV}$, respectively. $\Delta\gamma_1 \approx -0.2\text{eV}$ is the correction to the first nearest neighbor due to edge-distortion [12]. Applying a Taylor expansion to Eq. (1) the band structure of an armchair GNRs can be approximated by an effective mass model as:

$$\begin{aligned} E_n^\pm(k_x) &\approx \pm \left(\frac{E_{G,n}}{2} + \frac{(\hbar v_n k_x)^2}{E_{G,n}} \right) \\ &= \pm \left(\frac{E_{G,n}}{2} + \frac{\hbar^2 k_x^2}{2m_n^*} \right) \end{aligned} \quad (5)$$

where m_n^* is the effective mass of subband n and is given by:

$$m_n^* = \frac{E_{G,n}}{2v_n^2}. \quad (6)$$

Using the effective mass model, the density of states per unit length for n -th subband can be written as:

$$\begin{aligned} \rho_n(E) &= \frac{4}{2\pi} \left(\frac{\partial E}{\partial k} \right)^{-1} \\ &= \frac{\sqrt{2m_n^*} \Theta(E - E_{G,n}/2)}{\pi \hbar \sqrt{E - E_{G,n}/2}} \end{aligned} \quad (7)$$

3. Line-Edge Roughness Scattering

Using the Fermi-golden rule the transition rate of electrons due to line-edge roughness from subband n with an

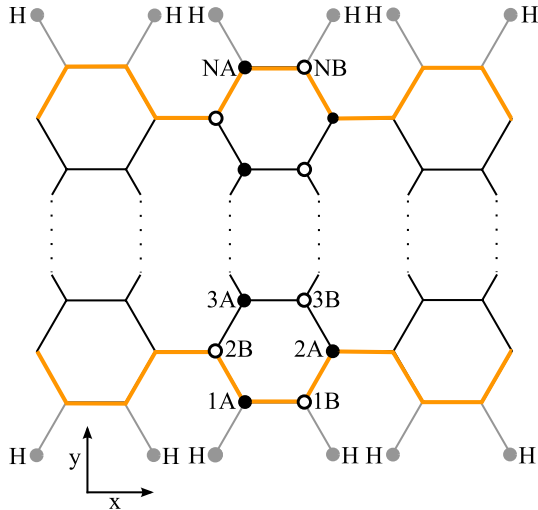


Figure 1: The structure of a GNR with armchair edges and the $x - y$ coordinate system. The edges of the GNR are terminated by hydrogen atoms

initial wave-vector k_x , represented by $|n, k_x\rangle$, to another subband n' with a final wave-vector k'_x , represented by $|n', k'_x\rangle$, can be written as:

$$\begin{aligned} \mathcal{S}_{n,n'}(k_x, k'_x) &= \\ \frac{2\pi}{\hbar} |\langle n', k'_x | H_{\text{LER}} | n, k_x \rangle|^2 &\delta(E_{n'}(k'_x) - E_n(k_x)) \end{aligned} \quad (8)$$

The delta function states the energy conservation, where line-edge roughness scattering is assumed to be an elastic process. Due to open boundaries in the longitudinal direction (x -axis) and confinement along the transverse direction (y -axis), the electron wave functions are given by:

$$\psi(x, k_x) = \langle x | n, k_x \rangle = \frac{1}{\sqrt{L}} \phi_n \exp(ik_x x). \quad (9)$$

Here L is the length of the ribbon. We assume that the band-edges of the ribbon are modulated by the width fluctuations due to line-edge roughness. Therefore, the perturbation potential is given by [13]:

$$\begin{aligned} H_{\text{LER}}(x) &= \delta E_{C,n} = -\frac{c}{W^2} \delta W \\ &= -\frac{\delta W(x)}{W} E_{C,n} \end{aligned} \quad (10)$$

$\delta W(x)$ denotes the width fluctuations and $W = \langle W(x) \rangle$ is the average width of the ribbon. The line edge roughness can be described by an auto correlation function as:

$$\begin{aligned} R(x_1, x_2) &= \langle \delta W(x_1) \delta W(x_2) \rangle \\ &= \Delta W^2 \exp\left(-\frac{|x|}{\Delta L}\right) \end{aligned} \quad (11)$$

ΔW is the root mean square of the fluctuation amplitude and ΔL is the roughness correlation which is a measure of smoothness. We assume two rough edges for the ribbon. Under the condition that the roughnesses of these two edges are uncorrelated, the transition rate can be obtained as:

$$\begin{aligned} \mathcal{S}_n(k_x, k'_x) &= \\ \frac{\pi E_{G,n}^2 \Delta W^2 \Delta L}{\hbar W^2 L (1 + q^2 \Delta L^2)} &\delta(E_{n'}(k'_x) - E_n(k_x)) \end{aligned} \quad (12)$$

Here $q = k_x - k'_x$. To obtain the conductance and the mean free path of GNRs the relaxation time due to line-edge roughness must be evaluated. Using Eq. (12) and $1/\tau_n(k_x) = \sum_{k'_x} \mathcal{S}_n(k_x, k'_x) (1 - \cos \alpha)$ the relaxation time for electrons in some subband n with a wave vector k_x is given by

$$\begin{aligned} \tau_n(E) &= \left(\frac{W}{\Delta W} \right)^2 \times \\ \frac{\hbar^2 (1 + 8m_n^*(E - E_{G,n}/2) \Delta L^2 / \hbar^2) \sqrt{E - E_{G,n}/2}}{2\sqrt{2}m_n^* E_{G,n}^2 \Delta L} \end{aligned} \quad (13)$$

where the summation runs over all final states k'_x , and α is the angle between the initial and final wave-vectors.

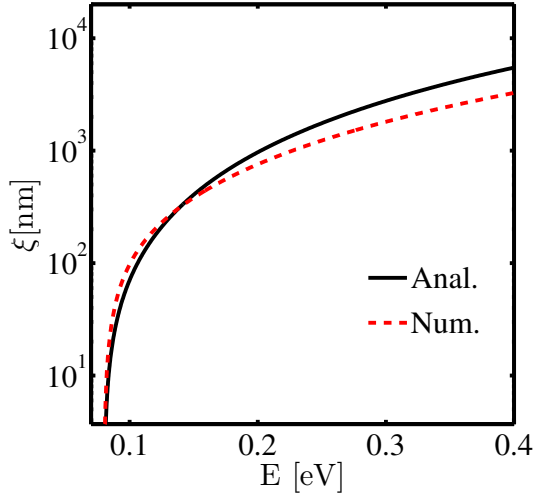


Figure 2: Comparison between the numerical results and the analytical models for the localization length as a function of energy for $E_F = 0.6E_C$, $\Delta L = 3\text{nm}$, $\Delta W = 0.3\text{nm}$, and $T = 300\text{K}$.

4. Localization of Carriers

In the absence of scattering, carrier transport is in the ballistic regime. In this regime the conductance is independent of the device length. In the presence of scattering, transport of carriers is in the diffusive regime, where the conductance is inversely proportional to the device length (L):

$$G(E) \approx G_0 \frac{1}{1 + L/\lambda(E)} \left(-\frac{\partial f}{\partial E} \right) \quad (14)$$

with $G_0 = 2q^2/h$. In this regime the mean free path of carriers can be defined as: $\lambda(E) = v_g(E)\tau(E)$ [14]. $v_{g,n} = \hbar^{-1} \partial E / \partial k = \sqrt{2(E - E_{C,n})/m_n^*}$ is the group velocity of the respective subband. However, in the presence of disorder the carrier wave packet can be scattered back and forth between potential barriers and standing waves along the device can develop. In this regime, referred to as localization regime, the transport of carriers takes place by tunneling between localized states and the conductance of the ribbon decreases exponentially with the ribbon's length [10]:

$$G(E) \approx G_0 \exp \left[-\frac{L}{\xi(E)} \right] \left(-\frac{\partial f}{\partial E} \right) \quad (15)$$

It has been shown that the localization length in quasi-one dimensional devices is related to the mean free path by [15]: $\xi_n(E) \approx N_{\text{ch}}(E)\lambda_n$, where $N_{\text{ch}}(E)$ denotes the number of active conducting channels at some energy E .

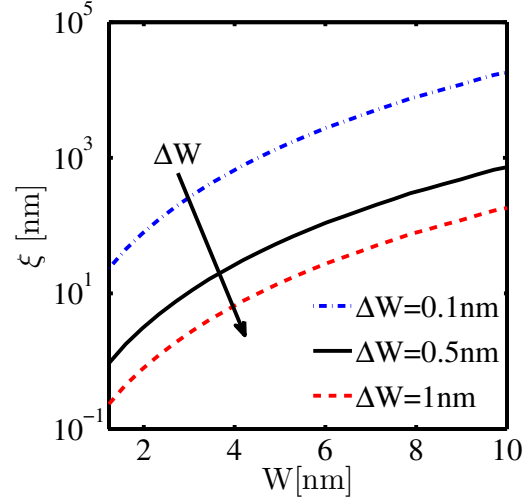


Figure 3: The localization length as a function of the GNR width for different roughness amplitudes ΔW for $\Delta L = 3\text{nm}$, $E_F = 0.6E_C$, and $T = 300\text{K}$

4.1. Localization Length and Mean Free Path

Using Eq. (13) and replacing $v_{g,n}$, the mean free path due to line-edge roughness scattering can be obtained as:

$$\lambda_n(E) = v_{g,n}(E)\tau_n(E) = \left(\frac{W}{\Delta W} \right)^2 \times \frac{\hbar^2 (1 + 8m_n^*(E - E_{G,n}/2)\Delta L^2/\hbar^2) (E - E_{G,n}/2)}{2m_n^*\Delta L E_{G,n}^2} \quad (16)$$

In a device with large splitting of the subbands and non-degenerate statistics the first subband contributes mostly to the total carrier transport, i.e. $N_{\text{ch}} = 1$. In this case one can approximate the localization length as $\xi(E) \approx \lambda(E)$. As shown in Fig. 2, the localization length is very small for carriers close to the conduction band and increases as the kinetic energy of the carrier increases.

If the ribbon has a large effective mass (narrow GNRs) or a large correlation length, the localization length and the mean free path scale as: $\lambda, \xi \propto W^2$, see Fig. 3.

The conductance of GNRs in the diffusive and localization regime is compared in Fig. 4 and Fig. 5 according to the geometrical parameters. Fig. 4 indicates that at the same width the localization of carriers is more pronounced in longer GNRs. Fig. 5 shows that at the same length the localization is more pronounced in narrower GNRs.

5. Conclusions

GNRs with band gaps suitable for electronic applications have a width below 10nm. In this regime line-edge roughness is the dominant scattering mechanism. Under this condition analytical models for the mean free path, and

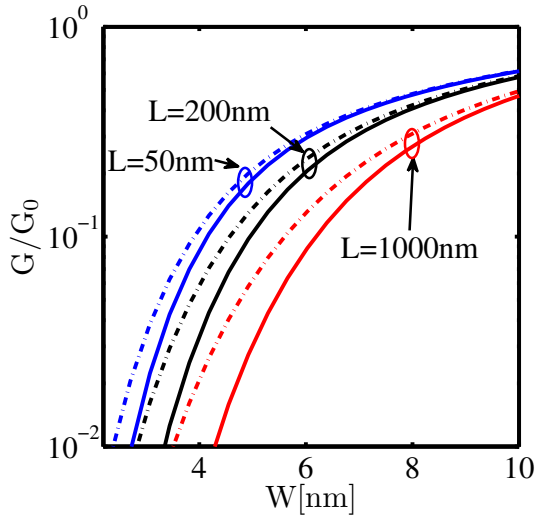


Figure 4: Comparison of conductance in the localization (solid-curves) and diffusive regime (dash-dot-curves) as a function of the width. $\Delta W = 0.5\text{nm}$, $\Delta L = 3\text{nm}$, $E_F = 0.6E_C$, and $T = 300\text{K}$

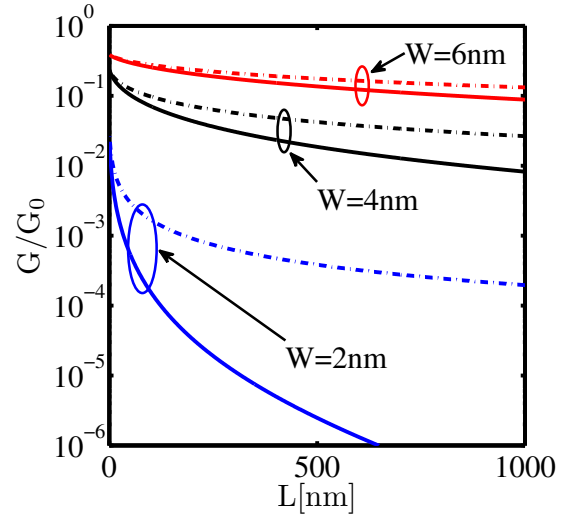


Figure 5: Comparison of conductance in the localization (solid-curves) and diffusive regime (dash-dot-curves) as a function of the length. $\Delta W = 0.5\text{nm}$, $\Delta L = 3\text{nm}$, $E_F = 0.6E_C$, and $T = 300\text{K}$

the localization length of carrier in GNRs are derived. Using these analytical models the dependences of the conductance and the localization length on the geometrical and roughness parameters are studied. Employing these models one can appropriately select the geometrical parameters for optimizing the performance of GNR based electronic devices.

Acknowledgments

This work, as part of the ESF EUROCORES program EuroGRAPHENE, was partly supported by funds from FWF, contract I420-N16.

References

- [1] K.S. Novoselov, A.K. Geim, S.V. Morozov, D. Jiang, Y. Zhang, S.V. Dubonos, I.V. Grigorieva, and A.A. Firsov. Electric Field Effect in Atomically Thin Carbon Films. *Science*, 306(5696):666–669, 2004.
- [2] A.K. Geim and K.S. Novoselov. The Rise of Graphene. *Nature Mater.*, 6(3):183–191, 2007.
- [3] I. Calizo, A.A. Balandin, W. Bao, F. Miao, and C.N. Lau. Temperature Dependence of the Raman Spectra of Graphene and Graphene Multilayers. *Nano Lett.*, 7(9):2645–2649, 2007.
- [4] K.S. Novoselov, A.K. Geim, S.V. Morozov, D. Jiang, M.I. Katsnelson, I.V. Grigorieva, S.V. Dubonos, and A.A. Firsov. Two-Dimensional Gas of Massless Dirac Fermions in Graphene. *Nature (London)*, 438(7065):197–200, 2005.
- [5] A.K. Geim and A.H. McDonald. Graphene: Exploring Carbon Flatland. *Phys. Today*, 60(8):35–41, 2007.
- [6] M.Y. Han, B. Özyilmaz, Y. Zhang, and P. Kim. Energy Band-Gap Engineering of Graphene Nanoribbons. *Phys. Rev. Lett.*, 98(20):206805 (4pp), 2007.
- [7] Y. G. Semenov, K. W. Kim, and J. M. Zavada. Spin Field Effect Transistor with a Graphene Channel. *Appl. Phys. Lett.*, 91(15):153105 (3pp), 2007.
- [8] Y. Zhang, Y. Tan, H. L. Stormer, and P. Kim. Experimental observation of the quantum Hall effect and Berry's phase in graphene. *Nature (London)*, 438:201–204, 2005.
- [9] Y. Yang and R. Murali. Impact of Size Effect on Graphene Nanoribbon Transport. *IEEE Electron Device Lett.*, 31(3):237–239, 2010.
- [10] S. Datta. *Electronic Transport in Mesoscopic Systems*. Cambridge University Press, New York, 1995.
- [11] Y. Son, M. L. Cohen, and S. G. Louie. Energy Gaps in Graphene Nanoribbons. *Phys. Rev. Lett.*, 97:216803(4pp), 2006.
- [12] D. Gunlycke and C. T. White. Tight-Binding Energy Descriptions of Armchair-Edge Graphene Nanostrips. *Phys. Rev. B*, 77:115116 (6pp), 2008.
- [13] T. Fang, A. Konar, H. Xingi, and D. Jena. Mobility in Semiconducting Graphene Nanoribbons: Phonon, Impurity, and Edge Roughness Scattering. *Phys. Rev. B*, 78(20):205403 (8pp), 2008.
- [14] D. J. Thouless. Localization Distance and Mean Free Path in One-Dimensional Disordered Systems. *J. Phys. C: Solid State Phys.*, 6:49–51, 1973.
- [15] N. Nemeč, D. Tomanek, and G. Cuniberti. Modeling Extended Contacts for Nanotube and Graphene Devices. *Phys. Rev. B*, 77(12):125420 (12pp), 2008.